Thermal performance of semitransparent CdTe BIPV window at temperate climate.

ALRASHIDI, H., GHOSH, A., ISSA, W., SELLAMI, N., MALLICK, T.K. and SUNDARAM, S.

2020

Thermal Performance of Semitransparent Cdte BIPV Window at Temperate Climate

Hameed Alrashidi[1, 2,*] Aritra Ghosh[1*], Walid Issa[3], Nazmi Sellami[4], Tapas. K. Mallick[1], Senthilarasu Sundaram[1*]
[1]Environment and Sustainability Institute, University of Exeter Penryn Campus, Penryn Cornwall, TR10 9FE, UK
[2]Kuwait Fund for Arab Economic Development, Mubarak Al-Kabeer St., Kuwait City, P.O. Box 2921 Safat 13030, Kuwait
[3]Sheffield Hallam University, City Campus, Sheffield, S1 1WB, UK
[4]School of Engineering, Robert Gordon University, Aberdeen, AB10 7JG, UK
Corresponding author: ha314@exeter.ac.uk

Abstract
Semi-transparent photovoltaic (PV) technology is attractive for building-integrated photovoltaics (BIPV) due to its ability to lower the admitted solar heat gain, to control the penetrating daylight and to generate onsite benevolent direct current power. In this work, semi-transparent cadmium telluride (CdTe) based BIPV as window was experimentally characterized using outdoor test cell in temperate UK climate. Spectral measurement confirmed its 25% visible transmission and 12% solar transmission. Thermal transmission and solar heat gain coefficient were calculated from measured thermal data. Overall heat transfer coefficient (*U*-value) of 2.7 W/m^{2}K was found for outdoor and indoor characterization of CdTe BIPV window. A comparison with single glazed window has been produced emphasis its feasibility for Facade buildings.

Highlights:

- Test cell characterization was performed to evaluate thermal performance of CdTe BIPV glazing.
- Visible transmission of this CdTe BIPV window is 25%
- Overall heat transfer coefficient of 2.7 W/m^{2}K was found for CdTe BIPV glazing.

Nomenclature	
A_g	Aperture area of glazing (m^2)
A_i	Anisotropy index
A_{wall}	Interior wall surface area (m^2)
C_{tc}	Heat capacity of air (kJ/kgK)
C_g	Heat capacity of water (kJ/kgK)
h_0	Heat transfer coefficient from test cell external surface to ambient (W/m^{2}K)
h_i	Heat transfer coefficient from test cell internal surface to interior of test cell (W/m^{2}K)
I	Incident solar radiation on the vertical surface of glazing (W/m^2)
$I_{beam,h}$	Incident beam solar radiation on the horizontal surface (W/m^2)
$I_{dif,h}$	Incident diffuse solar radiation on the horizontal surface (W/m^2)
I_{extra}	Incident extra-terrestrial solar radiation (W/m^2)
I_{sc}	Solar constant (W/m^2)
k_d	Diffuse factor
k_g	Extinction coefficient
k_T	Clearness index
K_{pl}	Thermal conductivity of polystyrene (W/mK)
K_{wd}	Thermal conductivity of wood (W/mK)
L_{pl}	Thickness of polystyrene (m)
L_{wd}	Thickness of wood (m)

M_{tc}	Mass of the air inside test cell (kg)
N_g	Number of glass pane
n	Refractive index
P	Power output from PV (W)
Q_{in}	Total energy incident on the glazing (W)
Q_{tc}	Total energy available inside the test cell (W)
Q_g	Heat through the glazing Incident solar radiation (W)
Q_{loss}	Heat loss through the surfaces of test cell (W)
r_h	Radius of heat exchanger pipe (m)
TSE	Transmitted solar energy through glazing (W/m^2)
$T_{tc,in}$	Interior temperature (^0C)
T_a	Ambient temperature (^0C)
U_g	Overall heat transfer coefficient of glazing (W/m^2K)
Greek symbols	
α	Absorptance
τ	Transmittance
τ_v	Vertical global transmittance
τ_{dir}	Direct transmittance
τ_{diff}	Diffuse transmittance
θ	Incidence angle

1. Introduction

Residential and commercial buildings consume close to 40% energy globally which comes from fossil fuels (International Energy Agency, 2018), which have an adverse environmental impact. Buildings consume energy primarily due to heating, cooling and lighting energy demand (Ghosh et al., 2019a; Ghosh and Norton, 2019) . Traditional single or double glazing are not highly thermally insulated which allow the transmission of a high amount of heat and allow external solar heat to indoor (Li et al., 2015). Presently new glazing material has been investigated to improve the heating and cooling loads in buildings (Ghosh et al., 2020, 2018a, 2017; Selvaraj et al., 2019). This will allow for more energy savings and boosting the efficiency of the future buildings. Figure 1 shows the detailed classification of advanced glazing technologies.

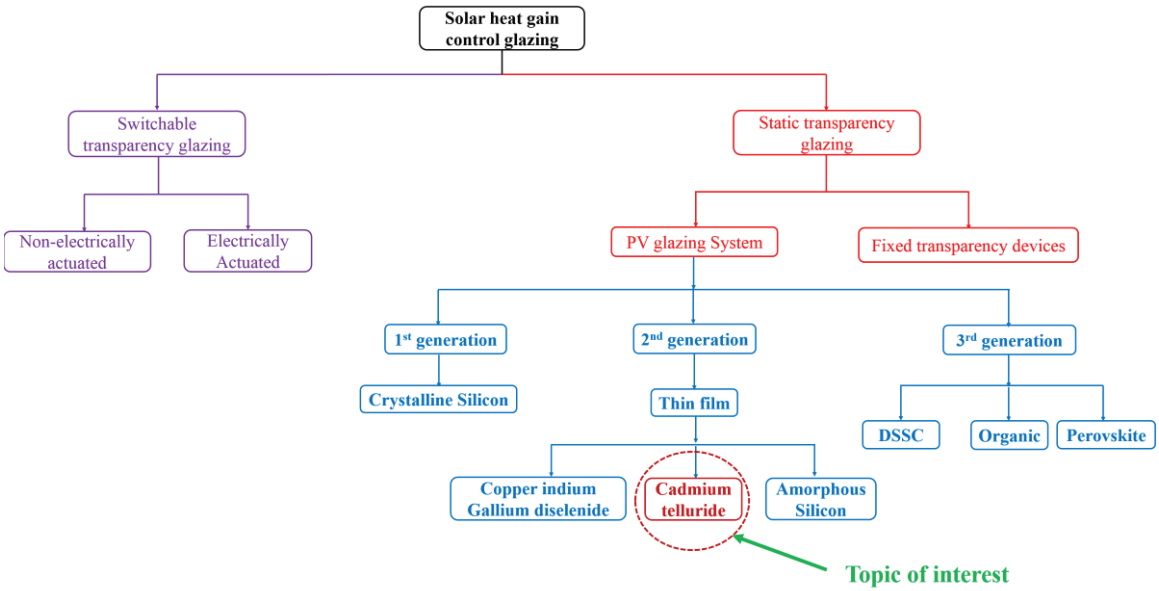

Fig 1. The different types of glazing technologies.

Glazing technologies can primarily be divided into switchable transparency glazing and static transparency glazing. Switchable transparency glazing can change their optical transmission from transparent to an opaque state by electrical or non-electrical actuation (Ghosh and Norton, 2018). For electrically powered switchable glazing, external stimulation is required to control the transparency (Ghosh et al., 2016a). Static transparent glazing includes aerogel (Zinzi et al., 2019), vacuum (Ghosh et al., 2016b), low-e coating, and photovoltaic (Saifullah et al., 2016; Skandalos and Karamanis, 2015) types.

Constant or static semi-transparent PV (BIPV) for buildings glazing integration is promising because they provide control over solar heat gain and daylight and generate benign electricity concomitantly (Saifullah et al., 2016). PV system in a BIPV glazing includes crystalline silicon (Ghosh et al., 2018b), thin film amorphous (Lu et al., 2017), cadmium telluride (CdTe) (Alrashidi et al., 2019) (Sun et al., 2018), copper indium gallium selenide (CIGS), DSSC (Selvaraj et al., 2019), perovskite (Ghosh et al., 2020), and organic (Chemisana et al., 2019) type. Crystalline silicone-based BIPV dominates the market because they have higher durability and efficiency (Green et al., 2019) . However, opaque nature crystalline silicon limits its own application for BIPV window. Thus, thin-film PV devices can be a suitable option.

Using space between crystalline PV cells, semi-transparent PV glazing was investigated where only PV performance was the primary investigating parameters (Park et al., 2010). Glazing factors were not included in that work. In another work spaced type, semi-transparent PV glazing was characterised for skylight application at Kovilpatti (9°10”0N, 77°52”0E), Tamil Nadu, for rooftop window and south facing wall application. Maximum daylight factor of 4% and indoor illuminance of 850 lux was obtained while 0.62 was (Karthick et al., 2018a) the PV coverage ratio. Solar factor was improved by 75% when coverage ratio was 0.69 (Karthick et al., 2018b).Using amorphous silicon (a-Si) based 40% transparent PV glazing was able to reduce electricity consumption by 55% (Miyazaki et al., 2005). Temperature can be reduced by using an optimized air gap for ventilated semi-transparent a-Si based BIPV window. At Berkeley climate, the air gap depth between 400 and 600 mm was beneficial to save 15% net electricity compared to 200 mm thick air gap which saved about 35% of electricity use per year than non-ventilated BIPV window (Lu et al., 2016). In Hong Kong climate, 23% and 28% reduction in the annual electricity consumption for cooling was possible when single- glazed and ventilated double-glazed PV windows were used (Chow et al., 2009).

Thin film CdTe is potential for PV application because of its direct energy band gap of 1.45 eV closely matches with solar spectrum, absorption coefficient in the visible part of the solar spectrum in the range of (10^4 -10^5) cm^{-1}. CdTe for BIPV roof (Kumar et al., 2019), grid integration (Ozden et al., 2017), light-soaking effect (Virtuani et al., 2011) has already been investigated. However, one of the holistic application of CdTe can be in the field of BIPV glazing for building’s window because of its semi-transparent nature.

Recently Sun et.al. (Sun et al., 2018) investigated application using combined optical (defined by a Bidirectional Scattering Distribution Function), electrical (Sandia Array Performance Model) and annual energy (EnergyPlus) model to evaluate the performance of an office equipped with 10% transparent CdTe BIPV window. Higher window to wall ratio (i.e.≥45%) was recommended for CdTe based BIPV window compared to a conventional double-glazed system and for specific case this CdTe BIPV window reduced up to 73% energy consumption. Glare was highly controlled due to low transmission value than that of a double glazing. Barman et.al. (Barman et al., 2018) investigated five different transparent CdTe BIPV system by optical and electrical measurement and employed them in simulation using climatic data to understand the impact of energy saving for buildings. It was prevailed that the lowest transmittent CdTe offered highest annual yield. In Brazil, rooftop and façade integrated CdTe PV system was applied to meet four floor office building. Both of PV roof and façade have increased cost compared to the traditional Balance-of-System (BoS) components however they are economically positive. Surplus energy was

suggested to explore for electric vehicles (Sorgato et al., 2018). Colour comfort analysis of CdTe BIPV window showed that they can allow correlated colour temperature in the range of 3000-3500K when the daylight source is between 4000K to 6500K and maintain colour rendering index higher than 90 (Liu et al., 2019).

In this work for the first-time thermal performance of CdTe based BIPV window is investigated using indoor and outdoor characterization. Results were compared with another similar dimension of single glazing. Overall heat transfer coefficient and solar heat gain will be investigated for CdTe BIPV

2. Experimental Set-up

2.1. Indoor characterization

One semitransparent CdTe BIPV window, as shown in Figure 2, was employed for the indoor characterization. Spectral measurement was performed using UV-Vis –NIR (Ghosh et al., 2019b) to find out the average transmission of this BIPV window for fenestration integration as shown in Figure 3. Average solar and visible transmission of this CdTe BIPV had 12% and 25% respectively. Transmission nature of CdTe closely matches with previously published related work (Sebastian and Sivaramakrishnan, 1992, 1991). One 86% transparent (solar transmission) single glazing was investigated for comparison.

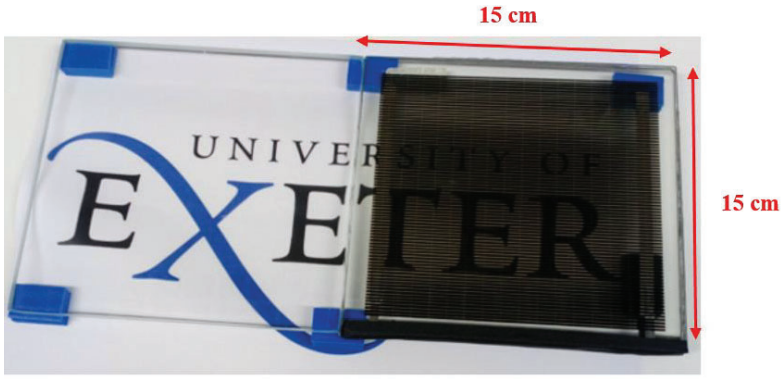

Fig 2. A photograph of single glazing and CdTe based semitransparent BIPV window

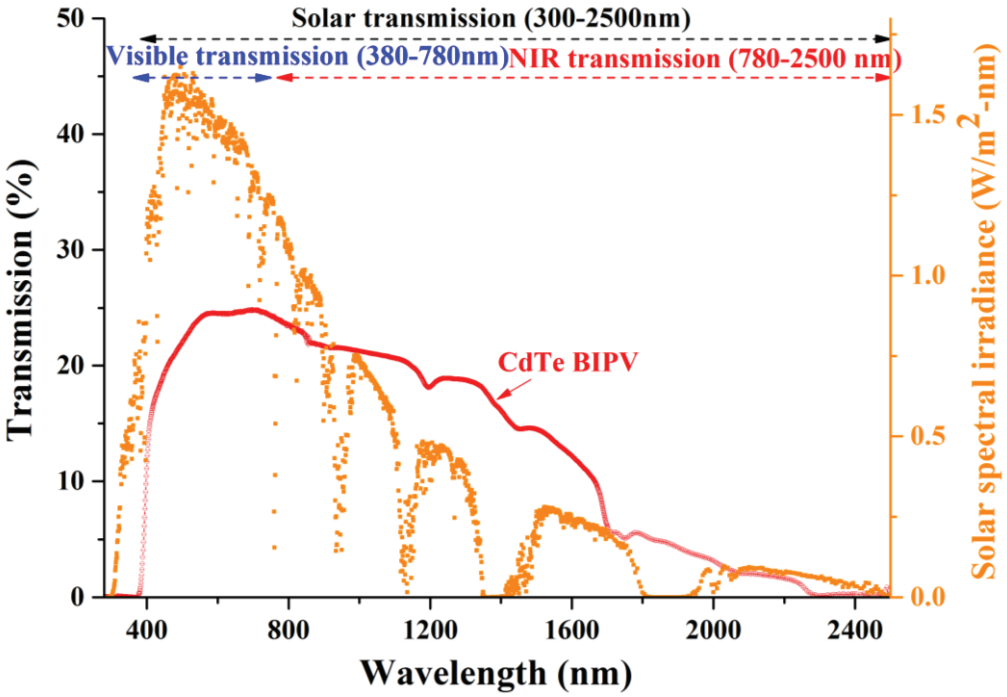

Figure 3: Total hemispherical transmission of CdTe based BIPV window

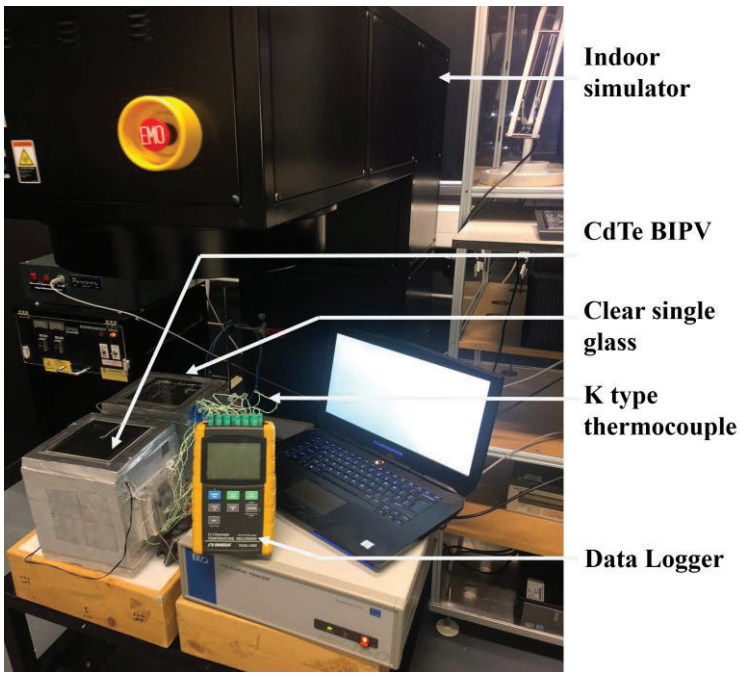

Figure 4: Photograph of indoor experimental setup

To perform thermal performance in an indoor controlled environment, experimental setup was fabricated as shown in Figure 4. A solar simulator (Class AAA+, AM 1.5) was employed as a source. Omega data logging system was used to record the temperatures of the inner and outer surfaces beside the inner room point. NI logging system was employed to measure power. The characterization was conducted under 1000

W/m^2 constant solar exposure for eight hours. Wind speed was represented by a fan delivering air at a speed of 1.5 m/s.

2.2. Outdoor characterization

To obtain thermal performance and glazing thermal factor (*U*-value and SHGC), outdoor characterisation was performed. Two test cells were designed, built, and installed at ESI building, Exeter University, Penryn, UK (50.16 N; -5.107 W). Each test cell had a dimension of 0.2 m × 0.2 m × 0.18 m and made of 0.025 m thick polystyrene sheets to provide improved insulation. Figure 5 and 6 show the schematic and photographic view of outdoor experimental setup.

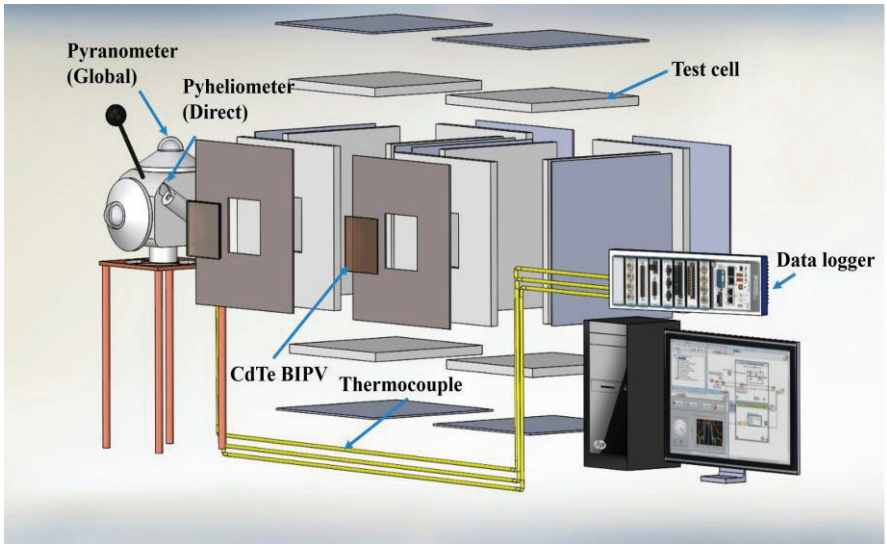

Figure 5. Schematic diagram of the outdoor experimental setup

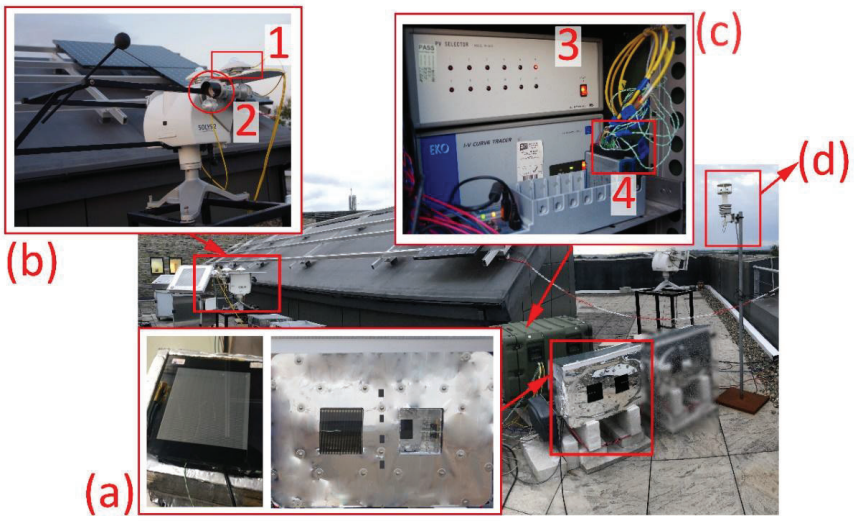

Figure 6. Full view of the experimental setup of two identical test cell with single-glazing and STPV glazing (a) Test cell with STPV and single-glazing (b.1) global and diffuse pyranometer (b.2) pyrheliometer (c.3) I-V tracer (c.4) NI data acquisition device (d) weather station

Six K-type thermocouple sensors were employed to monitor the temperatures of each test cell. The thermocouples were distributed as follows: one for the air temperature inside the insulated enclosure, one for the inside surface of the glass, and one for the outer surface of the single glazing or CdTe BIPV (based on the tested cell). Direct, diffuse, and global solar irradiances were recorded using Pyrheliometer and Pyranometer. The weather station was used to record ambient temperature and wind speed. Data acquisition and logging were achieved using NI9131 National instrument cDAQ.

3. Thermal performance

3.1. Solar heat gain coefficient

Solar heat gain coefficient (SHGC) measures the fraction of solar radiation that passes through the glazing as a fraction from vertical global solar radiation. Considering that the beam component of radiation being transmitted is at an incident angle (θ), the dynamic solar heat gain coefficient was calculated by equation 1 (Ghosh et al., 2016c):

$$SHGC = \frac{TSE}{I_{ver,global}} \tag{1}$$

Transmitted solar energy (TSE) through glazing (Waide and Norton, 2003) can be obtained as equation 2

$$TSE = \left(I_{beam,h} + I_{dif,h}A_i\right)\tau_{dir}r_b + I_{dif,h}\left(1+A_i\right)\tau_{dif,h}\frac{\left(1+\cos\beta\right)}{2} + I_{global}\rho_g\tau_g\frac{\left(1-\cos\beta\right)}{2} \tag{2}$$

where A_i is anisotropy index that indicates atmospheric transmittance due to beam solar radiation given by

$$A_i = \frac{I_{beam,h}}{I_{extra}} \tag{3}$$

The global solar transmittance through glazing τ_v was calculated (Waide and Norton, 2003) as given in equation 4.

$$\tau_v = \left[k_d\left\{k_T R_b\left(1-k_d\right)+\left(1-\cos\beta\right)\left(1-k_T\left(1-k_d\right)\right)\right\}+R_b\left(1-k_d\right)+R_g\frac{1-\cos\beta}{2}\right]\times \\ \tau_{dir}R_b\left(1-k_d\right)\left(1+k_d k_T\right)+\frac{\tau_{dif}k_d}{2}\left(1+\cos\beta\right)\left(1-k_T\left(1-k_d\right)\right)+\frac{\tau_g R_g\left(1-\cos\beta\right)}{2} \tag{4}$$

where

$$\tau = \frac{1}{2}\left[\frac{1-\left\{\frac{\sin\left(\theta-n\right)}{\sin\left(\theta+n\right)}\right\}^2}{1+\left(2n_g-1\right)\left\{\frac{\sin\left(\theta-n\right)}{\sin\left(\theta+n\right)}\right\}}+\frac{1-\left\{\frac{\tan\left(\theta-n\right)}{\tan\left(\theta+n\right)}\right\}^2}{1+\left(2n_g-1\right)\left[\frac{\tan\left(\theta-n\right)}{\tan\left(\theta+n\right)}\right]^2}\right]\times\exp\left(\frac{-k_g N_g t_g}{\cos\theta}\right) \tag{5}$$

and

$\tau = \tau_{dir}$ when $\theta = \theta_{dir}$

$\tau = \tau_{dif}$ when $\theta = \theta_{dif} = 59.68 - 0.1388\beta + 0.001497\beta^2$

$\tau = \tau_g$ when $\theta = \theta_g = 90 - 0.5788\beta + 0.002693\beta^2$

The diffuse factor (k_d) and clearness index (k_T) can be calculated by using equations 6 and 7.

$$k_d = \frac{I_{dif,h}}{I_{global}} \tag{6}$$

$$k_T = \frac{I_{global}}{I_{extra}} \tag{7}$$

where

$$I_{extra} = I_{sc}\left(1 + 0.033\cos\frac{360n}{365}\right)\left(\cos\phi\cos\delta\cos\omega + \sin\phi\sin\delta\right) \tag{8}$$

and I_{sc} is the solar constant , n is the day of year , ϕ is the latitude angle, δ is the declination angle and ω is the hour angle.

3.2. Overall heat transfer coefficient

To calculate overall heat transfer coefficient, following assumptions were made:

- Measurements were made while the glazing systems were in thermal steady state;
- Ground reflected solar radiation was assumed to be zero;
- The test cell was made of homogeneous highly insulating materials.

Energy balance equation using heat exchanger can be written as in equation 9

$$Q_{in} = Q_g + Q_{tc} + Q_{loss} + P \tag{9}$$

where

$$Q_{in} = I(t)A_g\tau_v(\theta)\alpha \tag{10}$$

The heat loss through the glazing is given by

$$Q_g = A_g U_g (T_{tc,in} - T_{tc,out}) \tag{11}$$

Q_{tc} is the heat stored in the test cell that is related to mass of air inside the test cell, heat capacity of air and variation of temperature with time and given by

$$Q_{tc} = M_{tc} C_{tc} \frac{dT}{dt} \tag{12}$$

The heat losses through the wall is represented by

$$Q_{loss} = Q_{wall} = (UA)_{wall}(T_{tc,in} - T_{tc,out}) \tag{13}$$

$$(UA)_{wall} = \left[\frac{1}{h_0} + \frac{L_{pl}}{K_{pl}} + \frac{L_{wd}}{K_{wd}} + \frac{1}{h_i} \right]^{-1} \times A_{wall} \tag{14}$$

The convective heat transfer coefficient between ambient air and outer glazing surface is calculated with the local wind speed V_{wind} as (Duffie and Beckman, 2013)(American society of heating refrigerating and air conditioning engineers, 1997)

$$h_i = 2.0 + 3\mathrm{V}_{\mathrm{wind}} \tag{15}$$

$$h_0 = 5.7 + 8.8\,\mathrm{V}_{\mathrm{wind}} \tag{16}$$

Overall heat transfer coefficient U_g for glazing with heat removal was calculated from

$$U_g = \frac{Q_{in} - Q_{tc} - Q_{loss} - P}{A_g(T_{tc,in} - T_{tc,out})} \tag{17}$$

Table 1 shows the Physical properties of materials used in the experiment for semitransparent CdTe BIPV

Table 1. Physical properties of materials used in the experiment for semitransparent CdTe BIPV

Parameters	Value
Temperature inside test cell ($T_{in,tc}$)	Measured by T type thermocouple (K)
Temperature outside test cell ($T_{out,tc}$)	Measured by T type thermocouple (K)
Aperture area of glazing ($A_{glazing}$)	0.0225 m^2
Internal volume of test cell (v_{air})	0.008 m^3
Mass of air inside test cell ($M_{tc} = v_{air} \times \rho_{air}$)	0.008 kg
Thickness of Polystyrene (L_{pl})	0.10 m
Thermal conductivity of polystyrene (K_{pl})	0.022 W/mK
Heat capacity of air (C_{air})	1.006 kJ/kgK

Density of air (ρ_{air})	1.2250 kg/m^3

4. Results and Discussion

4.1. Experimental results

Figure 7 exhibits the hourly clearness index and diurnal variation of CdTe surface, test cell and ambient temperature results were compared to a single glazing. Hourly clearness index (K_T) is the ratio of global horizontal solar radiation (I_{global}) and extra-terrestrial solar radiation (I_{extra}). Temperature of CdTe-BIPV internal surface was relatively higher than test cell temperature while reverse behavior was achieved for single glazing. This can be explained by thermal diffusivity and effusivity of glass and CdTe material as listed in Table 2.

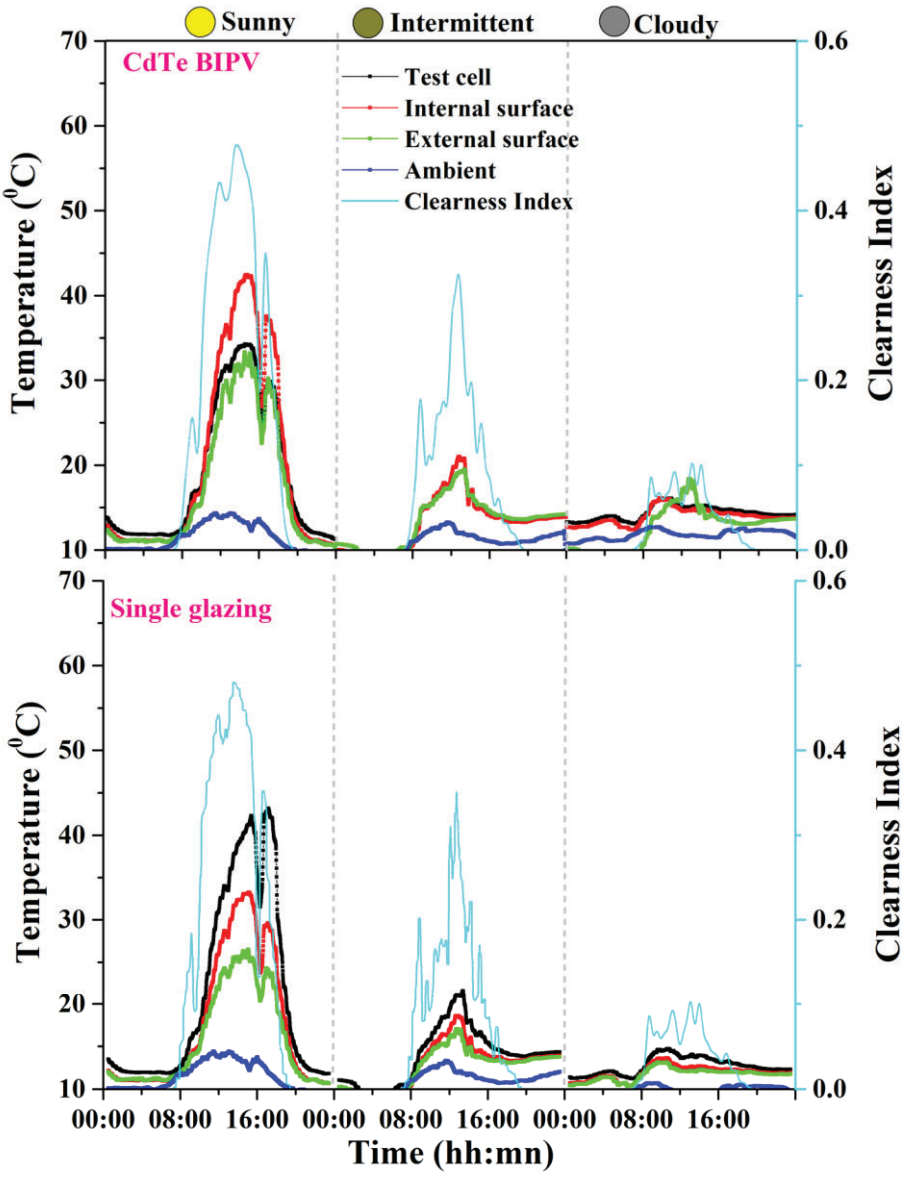

Figure 7: Diurnal variation of ambient temperature, test cell temperature, surface temperatures and clearness index in three different days for semi-transparent CdTe BIPV and single glazing

Table 2: Details of thermal diffusivity and thermal effusivity of CdTe and glass

Materials	Density (ρ) (kg/m^3)	Thermal conductivity (λ) (W/mK)	Heat capacity (C_p) (J/Kg/K)	Thermal diffusivity (m^2/s) $a = \frac{\lambda}{C_p \rho}$	Thermal effusivity $e = \sqrt{\lambda \rho C_p}$
CdTe	5860	5 (Su, 2016)	0.209	0.004	29.14
Glass	2203	1.38	703	8.9×10^{-7}	1461.9

Thermal effusivity is related to the ability of the material to absorb heat, while diffusivity is the speed to reach thermal equilibrium. The CdTe BIPV had two glass panes and CdTe material was sandwiched between them. Thus, enhanced heat flow and then reserved it in glass increased the internal glass temperature for CdTe BIPV while for single glass heat was transferred into the internal test cell. Very similar outcome was also found when experiment was performed in the indoor environment as shown in Figure 8. As shown, the interior surface temperature for the STPV sample is higher than the single glazed one. However, the test cell temperature was lower.

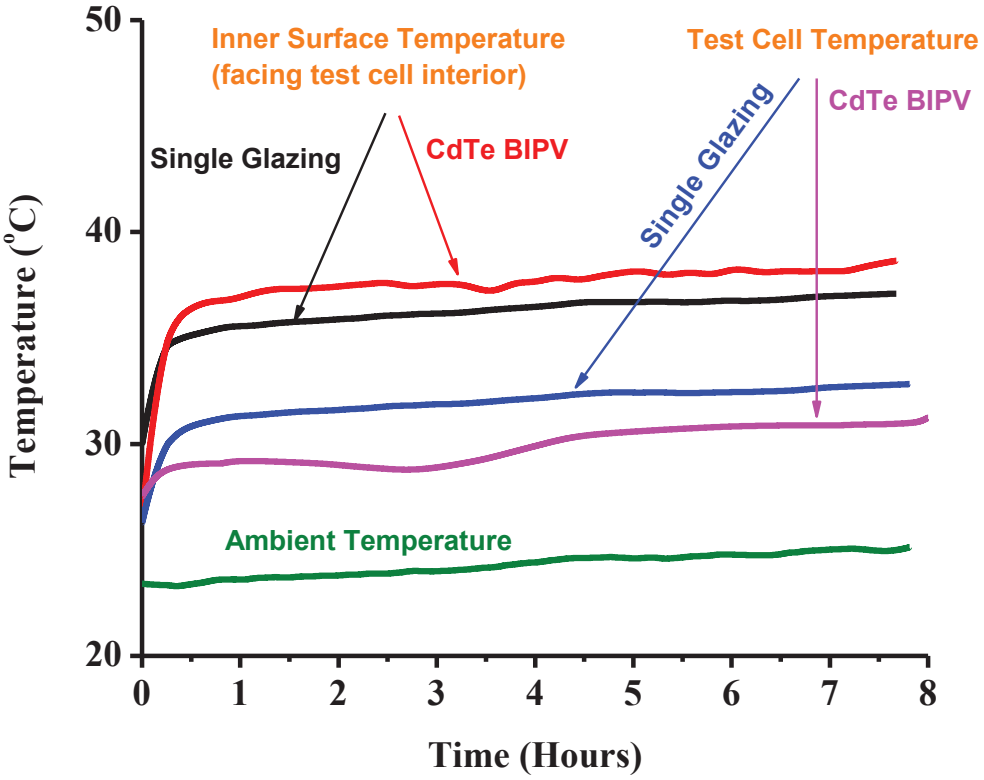

Figure 8: Variation of the internal glazing surface temperature and test cell internal temperature for CdTe BIPV and Single Glazing during indoor characterization.

4.2. Solar Heat Gain Coefficient

Figure 9 shows the variation of SHGC of CdTe BIPV for different incident angle. This CdTe BIPV had 20% SHGC mostly in the winter time. Change of SHGC in winter and summer was 70%. SHGC is the fraction of entering solar gain which is associated with direct, diffuse and reflected part of incident solar radiation on CdTe BIPV window. Direct solar radiation has strong correlation with incident angle which influenced to vary SHGC with incident angle. Maximum solar heat gain was possible to 20% while single glazing exhibited 72.8% maximum SHGC. Thus, for warm and hot climate this CdTe BIPV can save 73% solar gain and generate power concomitantly.

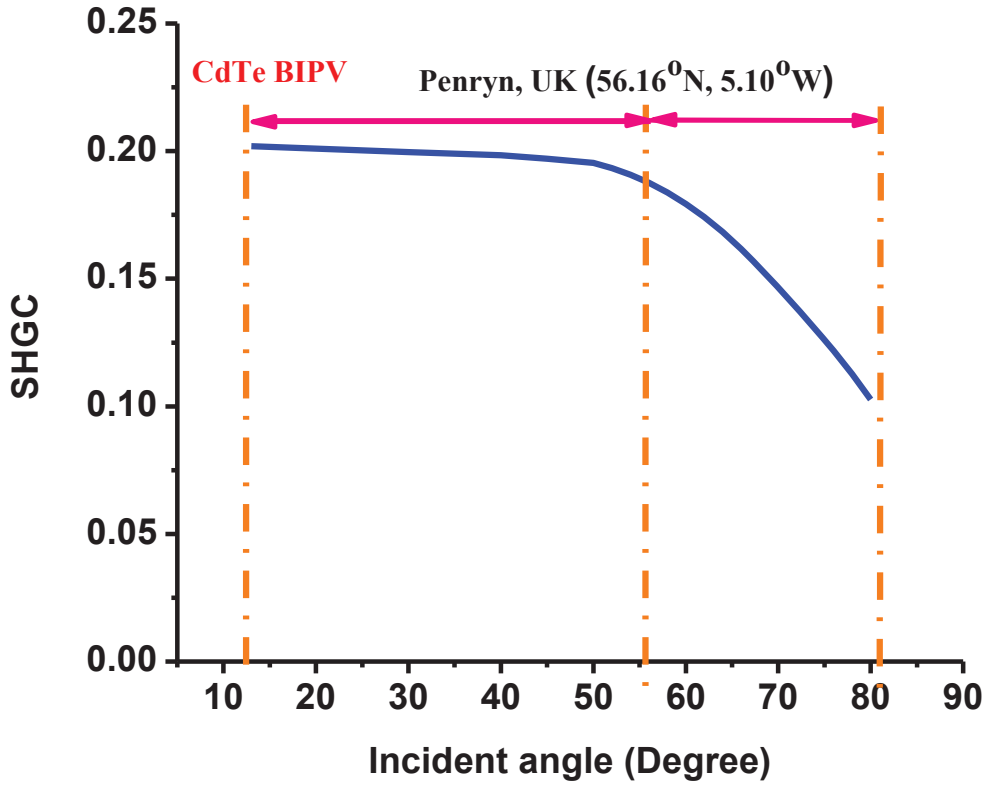

Figure 9: Variation of solar heat gain coefficient (SHGC) of CdTe BIPV window with different incident angle

4.3. Overall Heat Transfer Coefficient

Overall heat transfer coefficient was obtained for CdTe BIPV in outdoor and indoor conditions using equation 17 and shown in Figure 10 and 11 respectively. For indoor condition, single glazing's steady state was achieved after a short period rapidly compared with that of CdTe BIPV window.

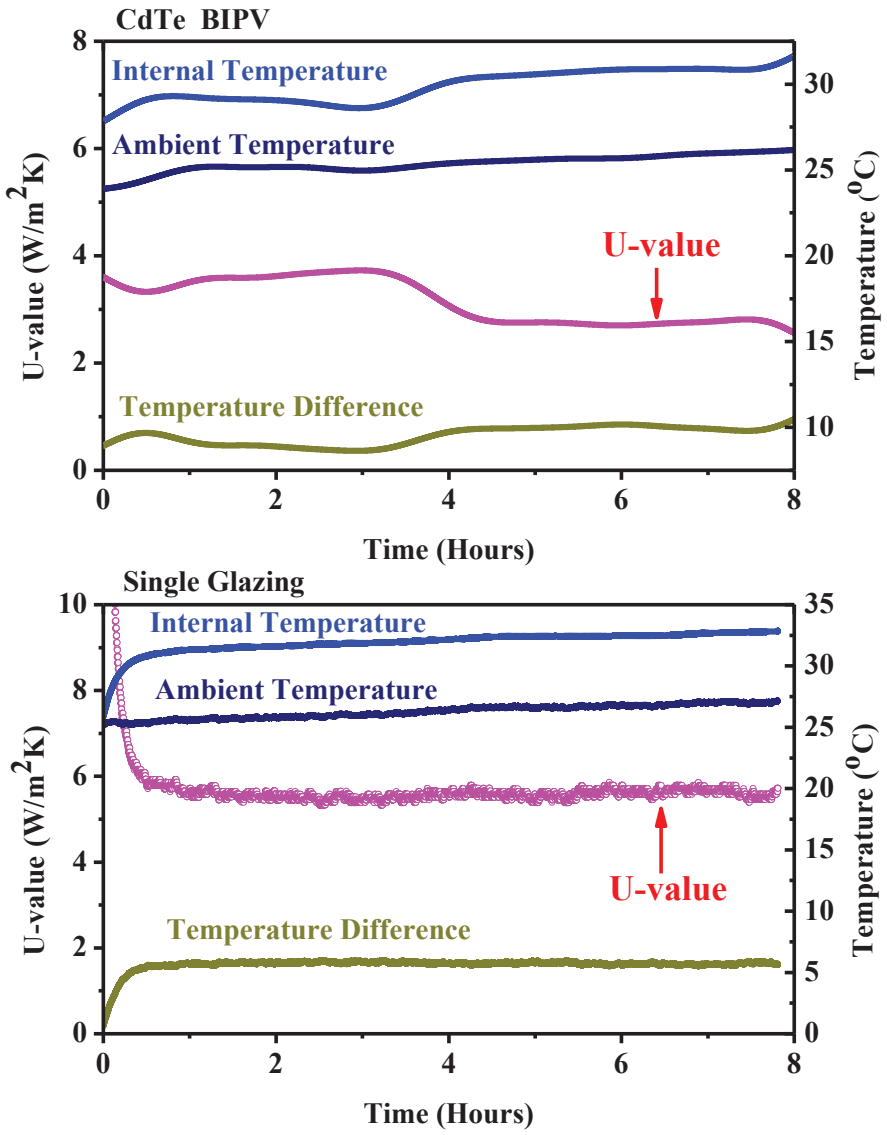

Figure 10: Calculated overall heat transfer coefficient (*U*-value), measured ambient temperature, test cell internal temperature and the temperature difference between ambient and test cell internal for (a) CdTe BIPV window (b) single glazing

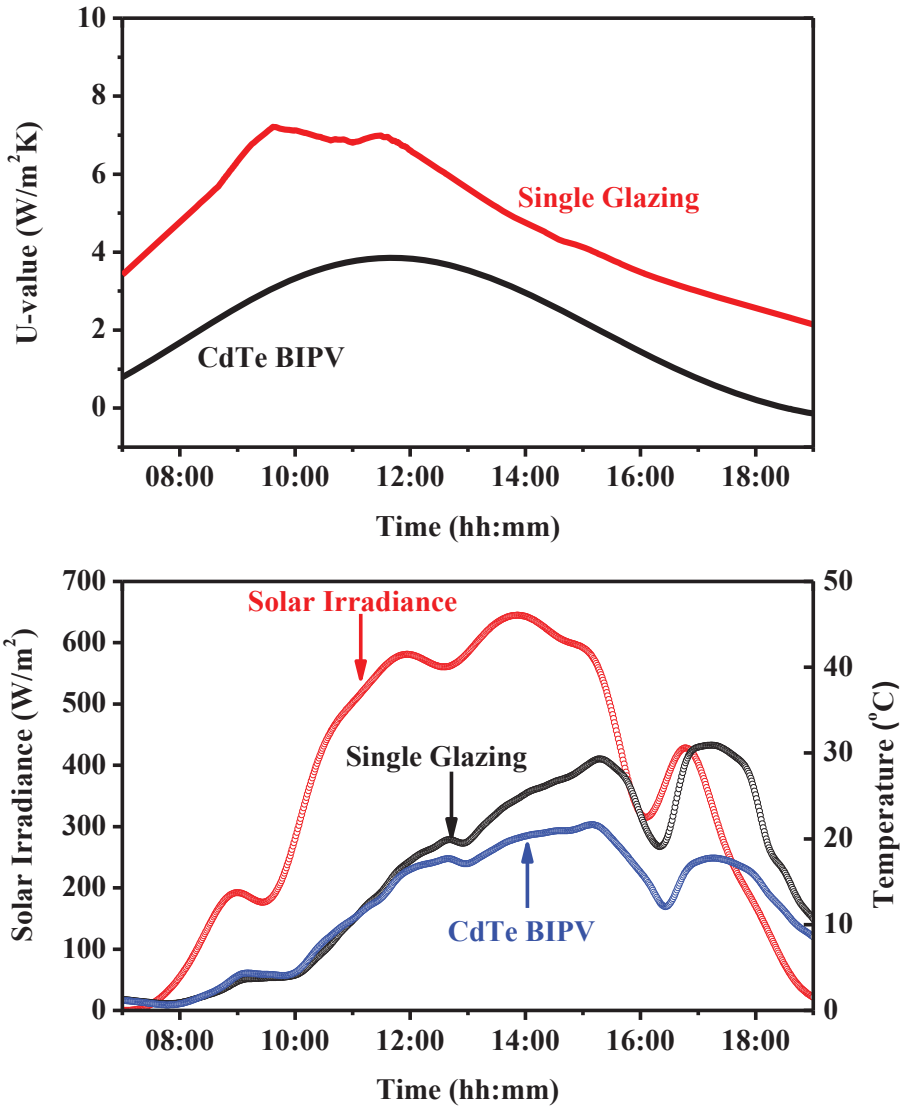

Figure 11. Diurnal Variation Solar irradiation and Temperature Difference for 25% Transparency STPV and single glazing test cells.

Table 3 summarizes the average *U*-values of the CdTe BIPV window and single glazing for indoor and outdoor conditions. The *U*-value of the CdTe BIPV was found to be identical with 2.7 W/m^{2}K for outdoor and indoor condition. Variation of indoor and outdoor condition was due to the fluctuating outdoor ambient. Variable wind speed and diurnal nature of external ambient made such variation. Results were compared to a single glazing and CdTe BIPV offered 37% lower heat loss than that of single glazing.

Table 3. Measured average *U*-values from indoor and outdoor experiments

Testing	CdTe BIPV Glazing	Single Glazing
Indoor Experiment	2.7 W/m^{2}K	5.7 W/m^{2}K
Outdoor Experiment	2.7 W/m^{2}K	5.6 W/m^{2}K

5. Conclusion

Thermal performance analysis of a CdTe BIPV window having dimension of 0.15 m × 0.15 m was investigated using indoor and outdoor test cell at temperate UK climate. Solar and visible transmission of this system was 12% and 25% respectively. Maximum solar heat gain from this CdTe BIPV window was found as 20% which was 73% lower than a 72.8% transparent single glazing. CdTe BIPV had an average *U*-value of 2.7 W/m^{2}K in the indoor and outdoor experiments. This average is lower than that of the single glazing that showed 5.7 W/m^{2}K in the indoor experiment and 5.6 W/m^{2}K in the outdoor experiment. Variations of the indoor and outdoor results are due to higher influence of uncontrolled external factors and disturbances in the outdoor condition. This study emphasis the usage of STPV in BIPV application to optimize the cooling or heating loads and to provide more electrical power.

Acknowledgement

This work is funded through PhD fellowship by Kuwait Fund for Development is greatly acknowledged. This work was also partially supported by EPSRC IAA grant achieved by Dr Aritra Ghosh.

References

Alrashidi, H., Issa, W., Sellami, N., Ghosh, A., Mallick, T.K., Sundaram, S., 2019. Performance Assessment of Cadmium Telluride-based Semi-Transparent Glazing for Power Saving in Façade Buildings. Energy Build. https://doi.org/10.1016/j.enbuild.2019.109585

American society of heating refrigerating and air conditioning engineers, 1997. 1997 ASHRAE Handbook: Fundamentals, ASHRAE handbook series. ASHRAE, Atlanta GA.

Barman, S., Chowdhury, A., Mathur, S., Mathur, J., 2018. Assessment of the efficiency of window integrated CdTe based semi-transparent photovoltaic module. Sustain. Cities Soc. 37, 250–262. https://doi.org/10.1016/j.scs.2017.09.036

Chemisana, D., Moreno, A., Polo, M., Aranda, C., Riverola, A., Ortega, E., Lamnatou, C., Domènech, A., Blanco, G., Cot, A., 2019. Performance and stability of semitransparent OPVs for building integration: A benchmarking analysis. Renew. Energy 137, 177–188. https://doi.org/10.1016/j.renene.2018.03.073

Chow, T.T., Pei, G., Chan, L.S., Lin, Z., Fong, K.F., 2009. A Comparative Study of PV Glazing Performance in Warm Climate. Indoor Built Environ. 18, 32–40. https://doi.org/10.1177/1420326X08100323

Duffie, J.A., Beckman, W.A., 2013. Solar Engineering of Thermal Processes: Fourth Edition, Solar Engineering of Thermal Processes: Fourth Edition. John Wiley & Sons, Inc., Hoboken, NJ, USA. https://doi.org/10.1002/9781118671603

Ghosh, A., Bhandari, S., Sundaram, S., Mallick, T.K., 2020. Carbon counter electrode mesoscopic ambient processed & characterised perovskite for adaptive BIPV fenestration. Renew. Energy 145, 2151–2158. https://doi.org/10.1016/j.renene.2019.07.119

Ghosh, A., Norton, B., 2019. Optimization of PV powered SPD switchable glazing to minimise probability of loss of power supply. Renew. Energy 131, 993–1001. https://doi.org/10.1016/j.renene.2018.07.115

Ghosh, A., Norton, B., 2018. Advances in switchable and highly insulating autonomous (self-powered) glazing systems for adaptive low energy buildings. Renew. Energy 126, 1003–1031. https://doi.org/10.1016/j.renene.2018.04.038

Ghosh, A., Norton, B., Duffy, A., 2017. Effect of sky conditions on light transmission through a suspended particle device switchable glazing. Sol. Energy Mater. Sol. Cells 160, 134–140. https://doi.org/10.1016/j.solmat.2016.09.049

Ghosh, A., Norton, B., Duffy, A., 2016a. First outdoor characterisation of a PV powered suspended particle device switchable glazing. Sol. Energy Mater. Sol. Cells 157, 1–9. https://doi.org/10.1016/j.solmat.2016.05.013

Ghosh, A., Norton, B., Duffy, A., 2016b. Measured thermal & daylight performance of an evacuated glazing using an outdoor test cell. Appl. Energy 177, 196–203. https://doi.org/10.1016/j.apenergy.2016.05.118

Ghosh, A., Norton, B., Duffy, A., 2016c. Behaviour of a SPD switchable glazing in an outdoor test cell with heat removal under varying weather conditions. Appl. Energy 180, 695–706. https://doi.org/10.1016/j.apenergy.2016.08.029

Ghosh, A., Norton, B., Mallick, T.K., 2018a. Daylight characteristics of a polymer dispersed liquid crystal switchable glazing. Sol. Energy Mater. Sol. Cells 174, 572–576. https://doi.org/10.1016/j.solmat.2017.09.047

Ghosh, A., Sarmah, N., Sundaram, S., Mallick, T.K., 2019a. Numerical studies of thermal comfort for semi-transparent building integrated photovoltaic (BIPV) -vacuum glazing system. Sol. Energy 190, 608–616. https://doi.org/10.1016/j.solener.2019.08.049

Ghosh, A., Sundaram, S., Mallick, T.K., 2019b. Colour properties and glazing factors evaluation of multicrystalline based semi-transparent Photovoltaic-vacuum glazing for BIPV application. Renew. Energy 131, 730–736. https://doi.org/10.1016/j.renene.2018.07.088

Ghosh, A., Sundaram, S., Mallick, T.K., 2018b. Investigation of thermal and electrical performances of a combined semi- transparent PV-vacuum glazing. Appl. Energy 228, 1591–1600. https://doi.org/10.1016/j.apenergy.2018.07.040

Green, M.A., Hishikawa, Y., Dunlop, E.D., Levi, D.H., Hohl-Ebinger, J., Yoshita, M., Ho-Baillie, A.W.Y., 2019. Solar cell efficiency tables (Version 53). Prog. Photovoltaics Res. Appl. 27, 3–12. https://doi.org/10.1002/pip.3102

International Energy Agency, 2018. Statistics and Data [WWW Document]. URL https://www.iea.org/

Karthick, A., Kalidasa Murugavel, K., Kalaivani, L., 2018a. Performance analysis of semitransparent photovoltaic module for skylights. Energy 162, 798–812. https://doi.org/10.1016/j.energy.2018.08.043

Karthick, A., Kalidasa Murugavel, K., Kalaivani, L., Saravana Babu, U., 2018b. Performance study of building integrated photovoltaic modules. Adv. Build. Energy Res. 12, 178–194. https://doi.org/10.1080/17512549.2016.1275982

Kumar, N.M., Sudhakar, K., Samykano, M., 2019. Performance evaluation of CdTe BIPV roof and façades in tropical weather conditions. Energy Sources, Part A Recover. Util. Environ. Eff. 0, 1–15. https://doi.org/10.1080/15567036.2019.1602216

Li, D., Li, Z.W., Zheng, Y.M., Liu, C.Y., Lu, L.B., 2015. Optical performance of single and double glazing units in the wavelength 337-900 nm. Sol. Energy 122, 1091–1099. https://doi.org/10.1016/j.solener.2015.10.028

Liu, D., Sun, Y., Liu, X., Wilson, R., Wu, Y., 2019. Evaluation of the colour properties of CdTe PV windows. Energy Procedia 158, 3088–3093. https://doi.org/10.1016/j.egypro.2019.01.1000

Lu, L., Zhang, W., Selkowitz, S.E., Yang, H., Curcija, D.C., Peng, J., 2016. Numerical investigation of the

energy saving potential of a semi-transparent photovoltaic double-skin facade in a cool-summer Mediterranean climate. Appl. Energy 165, 345–356. https://doi.org/10.1016/j.apenergy.2015.12.074

Lu, T., Li, X., Li, N., Peng, J., Yang, H., Wang, C., Wang, M., 2017. Comparison of energy performance between PV double skin facades and PV insulating glass units. Appl. Energy 194, 148–160. https://doi.org/10.1016/j.apenergy.2017.03.019

Miyazaki, T., Akisawa, A., Kashiwagi, T., 2005. Energy savings of office buildings by the use of semi-transparent solar cells for windows. Renew. Energy 30, 281–304. https://doi.org/10.1016/j.renene.2004.05.010

Ozden, T., Akinoglu, B.G., Turan, R., 2017. Long term outdoor performances of three different on-grid PV arrays in central Anatolia ??? An extended analysis. Renew. Energy 101, 182–195. https://doi.org/10.1016/j.renene.2016.08.045

Park, K.E., Kang, G.H., Kim, H.I., Yu, G.J., Kim, J.T., 2010. Analysis of thermal and electrical performance of semi-transparent photovoltaic (PV) module. Energy 35, 2681–2687. https://doi.org/10.1016/j.energy.2009.07.019

Saifullah, M., Gwak, J., Yun, J.H., 2016. Comprehensive review on material requirements, present status, and future prospects for building-integrated semitransparent photovoltaics (BISTPV). J. Mater. Chem. A 4, 8512–8540. https://doi.org/10.1039/C6TA01016D

Sebastian, P.J., Sivaramakrishnan, V., 1992. CdSe thin films as solar control coatings. Sol. Energy Mater. Sol. Cells 27, 321–326. https://doi.org/10.1016/0927-0248(92)90093-5

Sebastian, P.J., Sivaramakrishnan, V., 1991. Thin Solid Films, 202 (1991) 1-9 202, 1–9.

Selvaraj, P., Ghosh, A., Mallick, T.K., Sundaram, S., 2019. Investigation of semi-transparent dye-sensitized solar cells for fenestration integration. Renew. Energy 141, 516–525. https://doi.org/10.1016/j.renene.2019.03.146

Skandalos, N., Karamanis, D., 2015. PV glazing technologies. Renew. Sustain. Energy Rev. 49, 306–322. https://doi.org/10.1016/j.rser.2015.04.145

Sorgato, M.J., Schneider, K., Rüther, R., 2018. Technical and economic evaluation of thin-film CdTe building-integrated photovoltaics (BIPV) replacing façade and rooftop materials in office buildings in a warm and sunny climate. Renew. Energy 118, 84–98. https://doi.org/10.1016/j.renene.2017.10.091

Su, C., 2016. Thermal conductivity , electrical conductivity , and thermoelectric properties of CdTe o and Cd0 . 8Zn0 . 2Te crystals between room temperature and 780 C Thermal conductivity , electrical conductivity , and thermoelectric properties of CdTe and Cd 0 . 8 Z 057118, 0–10. https://doi.org/10.1063/1.4921025

Sun, Y., Shanks, K., Baig, H., Zhang, W., Hao, X., Li, Y., He, B., Wilson, R., Liu, H., Sundaram, S., Zhang, J., Xie, L., Mallick, T., Wu, Y., 2018. Integrated CdTe PV glazing into windows: energy and daylight performance for different architecture designs. Appl. Energy 231, 972–984. https://doi.org/10.1016/j.apenergy.2018.09.133

Virtuani, A., Mullejans, H., Dunlop, E.D., 2011. Comparison of indoor and outdoor performance measurements of recent commercially available solar modules. Prog. Photovolt Res. Appl. 15, 11–20. https://doi.org/10.1002/pip

Waide, P.A., Norton, B., 2003. Variation of insolation transmission with glazing plane position and sky conditions. Trans. Am. Soc. Mech. Eng. J. Sol. Energy Eng. 125, 182–189. https://doi.org/10.1115/1.1563630

Zinzi, M., Rossi, G., Anderson, A.M., Carroll, M.K., Moretti, E., 2019. Optical and visual experimental

characterization of a glazing system with monolithic silica aerogel. Sol. Energy 183, 30–39. https://doi.org/10.1016/j.solener.2019.03.013